



**Fermilab**

TM-1399  
2510.000  
2515.000  
2520.000

A SILICON DETECTOR READOUT SYSTEM  
USING COMMERCIALY AVAILABLE ITEMS

Dan Green

May 1986

## A. Physics of Silicon Detectors

The properties of silicon microstrip detectors (SMD) have been extensively reviewed elsewhere<sup>1)</sup>. In this note the basic properties are briefly noted.

### 1) Bulk Properties

The Einstein relation between the diffusion coefficient  $D$  and the mobility  $\mu$  is:

$$kT = qD/\mu \quad 1)$$

where  $q$  is the electron charge, and  $kT$  is proportional to the thermal energy. For silicon the electron mobility is  $\mu_e \sim 1400 \text{ cm}^2/\text{V}\cdot\text{sec}$  while the hole mobility is  $\mu_h \sim 500 \text{ cm}^2/\text{V}\cdot\text{sec}$ . The energy gap is  $E_g = 1.12 \text{ eV}$ . The intrinsic density of charge carriers at  $300^\circ\text{K}$  is  $n_i \sim 10^{11} \text{ cm}^{-3}$ . The doped conductivity obeys  $n_i p_i = np$ , which for typical doping yields a resistivity  $\rho$  (related to charge  $q$ , mobility  $\mu$ , and density  $n$ )

$$\rho = 1/q\mu n \quad 2)$$

of  $\rho_i \sim 200 \text{ K } \Omega\cdot\text{cm}$ ,  $\rho_n \sim 20 \text{ K } \Omega\cdot\text{cm}$ .

Charge is typically collected over a depletion depth  $d = 300 \text{ } \mu\text{m}$ . The density of Si is  $2.33 \text{ gm/cm}^3$ , and the radiation length  $x_0$  is  $9.36 \text{ cm}$ . A depth of  $300 \text{ } \mu\text{m}$  is  $6.6 \times 10^{-4}$  of an interaction length  $\lambda_I$ ,  $3 \times 10^{-3}$  of  $x_0$ , and causes an energy loss of  $116 \text{ keV}$ . The energy to liberate a pair is  $3.62 \text{ eV}$  which means  $32,000$  pairs in  $300 \text{ } \mu\text{m}$  or  $5.1 \text{ fC}$  of charge,  $Q_g$ , to collect.

### 2) Electrical Properties

The dielectric constant of Si is  $\epsilon = 1.05 \text{ pf/cm}$  or  $11.9 \epsilon_0$ . The relationship between  $V$  and  $I$  at a junction is

$$I(V) = I_0 (e^{qV/kT} - 1) \quad 3)$$

From this relation the forward junction resistance is  $R_F = (dI/dV)^{-1} = kT/qI$ . For  $300^\circ\text{K}$  at  $I = 1 \text{ ma}$ , then  $R_F = 25 \Omega$ . The reverse current  $I_0$  is difficult to calculate from first principles.

Application of a reverse voltage  $V_D$  to the junction results in a depletion region containing only fixed ions. The extent of this region can be calculated using electrostatics;  $\vec{\nabla} \cdot \vec{E} = \rho/\epsilon = dE/dz = qn/\epsilon$ . Then  $E = (qn/\epsilon)z$  and since  $\vec{E} = -(\vec{\nabla}V) = -dV/dz$ ,  $V = qnz^2/2\epsilon$ . For a depletion voltage  $V_D$

$$V_D = \frac{qnz_D^2}{2\epsilon} = z_D^2/2\epsilon\rho\mu \quad 4)$$

For example, full depletion  $d = z_D = 300 \mu\text{m}$  requires, (if  $\rho = 6 \text{ K}\Omega\cdot\text{cm}$ ,  $\mu = \mu_e$ ) that  $V_D = 51 \text{ V}$ . The capacity of this depletion region per unit area is  $\sim \epsilon/z_D$ . For  $z_D = d$ ,  $\epsilon/d$  is  $35 \text{ pf/cm}^2$ . A strip of  $50 \mu\text{m}$  pitch  $5 \text{ cm}$  long has a source capacity  $C_s \sim 0.9 \text{ pf}$ . Thus the source capacity is small for silicon strip detectors and is dominated by stray input lead capacity.

### 3) Longitudinal Charge Collection

Suppose the detector is fully depleted, then  $z_D = d$  or  $V_D = d^2/2\epsilon\rho\mu$ . In this case

$$E(z) = \left(\frac{2V_D}{d^2}\right) z \quad 5)$$

The velocity of charge motion is  $dz/dt = \mu E(z)$ . Integrating this equation of motion

$$z(t) = d e^{-t/t_c} \quad 6)$$

where the charge collection time  $t_c$  is

$$t_c = (d^2/2V_D\mu) \quad 7)$$

This equation can be thought of crudely as motion in a field  $\sim V_D/d$  of  $\sim 3.3 \text{ kV/cm}$ . The velocity is roughly  $\sim (V_D/d)\mu \sim 4.7 \times 10^6 \text{ cm/sec}$ . Over a distance  $\sim d/2$  the electron charge is collected in a time  $t_c \sim (d/2)/(V_D/d)\mu \sim 3.2 \text{ nsec}$ .

Assuming uniform ionization deposition, the collected charge and current go as

$$i(t) = \frac{Q_s}{t_c} e^{-t/t_c} \quad 8)$$

$$Q(t) = Q_s(1 - e^{-t/t_c}) \quad 9)$$

For  $Q_s = 5.1$  fC and  $t_c = 9.0$  nsec (holes), the initial hole current is  $i(0) = Q_s/t_c = 0.57$   $\mu$ A.

#### 4) Transverse Charge Collection

During drift toward the pickup electrode, the charge carriers diffuse. The distribution in a transverse coordinate  $y$  is gaussian with rms.

$$\sigma_y \approx \sqrt{2D_h t} \quad 10)$$

As a rough approximation, using  $t \sim t_c$  and equation 1 for  $D$ ,

$$\sigma_y \sim d \sqrt{\frac{kT}{qV_D}} \quad 11)$$

For  $qV_D = 100$  eV, at  $300^\circ\text{K}$  then  $\sigma_y \sim 4.7$   $\mu$ m or  $\sigma_y/d \sim 0.016$ . This implies that diffusion may be relevant to charge sharing between strips for small pitch detectors.

#### B. Noise In Front End Amplifiers

There are two general noise sources, thermal noise and shot noise<sup>2)</sup>. Per unit frequency interval  $d\omega$  the rms. noise currents are

$$i_T^2 = \frac{2kT}{\pi R} d\omega \quad 12)$$

$$i_s^2 = \frac{qI}{\pi} d\omega \quad 13)$$

Assume a source capacity  $C_s$ , source resistance  $R_s$ , and source charge drive  $Q_s$ . The front end amplifier has a gain  $A$  and time constant (low and high pass) of  $\tau$ .

$$f(\omega) = A \left[ \frac{\omega\tau}{1 + (\omega\tau)^2} \right] \quad 14)$$

The amplifier inputs are characterized<sup>3)</sup> by thermal noise due to  $R_s$ , shot noise due to a standing current  $I_B$  and thermal noise due to input impedance  $g_m = qI_E/kT = 1/R_B$  (see equation 3). Assuming currents sink into  $C_s$  and not  $R_s$ , the rms voltage noise is

$$\overline{v^2} = \overline{i_T^2} Z_{Cs}^2 + \overline{i_s^2} Z_{Cs}^2 + \overline{i_T^2} R_B^2 \quad (15)$$

$$= \left[ \frac{2kT}{\pi R_s (\omega C_s)^2} + \frac{qI_B}{\pi (\omega C_s)^2} + \frac{2kT}{\pi g_m} \right] d\omega \quad (16)$$

Convoluting  $\overline{v^2}$  with  $f(\omega)$  yields the noise sources modified by the amplifier.

$$\langle v^2 \rangle = \int_0^\infty |f(\omega)|^2 \overline{v^2} d\omega \quad (17)$$

$$\langle v^2 \rangle = A^2 \left[ \left( \frac{kT}{2R_s} + \frac{qI_B}{4} \right) \frac{\tau}{C_s^2} + \frac{kT}{2g_m \tau} \right] \quad (18)$$

The voltage amplifier output due to the source charge will be  $(Q_s A / C_s) e^{-1}$  where  $e^{-1}$  is due to  $f(\omega)$  if the shaping is matched to  $t_c$  ( $\tau - t_c$ ). The definition of the equivalent noise charge, ENC, due to noise is  $(A \text{ ENC} / C_s e)^2 = \langle v^2 \rangle$ . The ENC is typically thought of as consisting of series and parallel parts which are folded in quadrature.

$$(\text{ENCP})^2 = e^2 \left( \frac{kT}{2R_s} + \frac{qI_B}{4} \right) \tau \quad (19)$$

$$(\text{ENCs})^2 = e^2 \left( \frac{kT}{2g_m \tau} \right) C_s^2 \quad (20)$$

The series noise is proportional to the source capacity. For low source capacity (as with silicon),  $ENC \sim ENCP$ . For example,  $Q_s \sim 5.1 \text{ fC} \sim 32,000 \text{ q}$ . The ENCS due to  $g_m^{-1} \sim 25 \Omega$  at 1 mA with  $\tau = t_c \sim 10 \text{ nsec}$  shaping and  $C_s \sim 30 \text{ pf}$  stray capacity is 1125 q. Taking an input impedance of  $R_s = 1 \text{ M}\Omega$  and base current of 1  $\mu\text{A}$ , yields  $ENCP = 825 \text{ q}$ . Thus the signal to noise is  $\sim Q_s / \sqrt{ENC^2 + ENCP^2} = 23$ .

### C. Detectors

Detectors have lately become commercially available from a variety of sources. There exists a variety of available pitches and fanout schemes. It appears that at Fermilab, Micron<sup>4)</sup> is as near to a standard as can be found. These detectors are used by E691 and E687, for example, as well as others.

It is assumed that the detector strips are fanned out to a connector. For example Micron design L is 5 cm x 5 cm with 688 channels mixed between 25  $\mu\text{m}$  and 50  $\mu\text{m}$  pitch. The fanout is on Kapton to a receptacle 2.54 cm wide. The 1/10" centers of this receptacle are organized as 4 channels wide by 32 channels long. A typical card cage for this connector is shown in Figure 1. The design is that used in E-691 at Fermilab for the MSD2 preamp modified for the longer MSP1 thick film hybrid, which has identical pinouts.

### D. Preamp

A great variety of preamps exists for silicon detectors. On the basis of some comparative tests, a preferred preamp<sup>5)</sup> was chosen. The dimensions are shown in Figure 2. This preamp, the CERN MSP1, is compatible with the detector and card cage shown previously. It too is available commercially.

The ENC is quoted to be  $\sim 1040 \text{ q}$  for short gate widths (140 nsec) and  $C_s = 20 \text{ pf}$ . The input impedance is 1K  $\Omega$ , while the output is differential. The shaping time is  $\sim 70 \text{ nsec}$ . Power dissipation is 55 mW/channel.

Bench tests of the MSP1 were made by injecting 8 nsec input pulses. Supply voltages were  $\pm 5V$ . The current gain (single ended into 50  $\Omega$ ) was 1000. This gain is  $\sim 30$  times that of the CERN MSD2 preamp. That means that an input signal of 100 nA (5 fC in 50 nsec) will give outputs of  $\pm 5$  mV into 50  $\Omega$ . Such a signal is large enough that extensive RF shielding of the cable beyond the first preamp stage is unnecessary. The noise of the preamp is  $\leq 10$  nA referred to the input. The rise time is  $\sim 5$  nsec. The output is bipolar up to 40 mV output.

The differential outputs of the MSP1 make it ideal for fanning out away from the congested SMD region. A schematic of a remote amplifier and discriminator is shown in Figure 3. Ordinary unshielded twist and flat cable is perfectly adequate as a fanout cable. For example, the Fermilab standard Nano N-277C could be used as the final amplifier and discriminator. The MSP1 is well matched to the  $\pm 0.25$  mV input threshold limit of this unit. In fact, the operation of this complete system was found to be quite painless.

#### E. Test Results

A test setup was constructed as shown in Figure 4. A  $Sr^{90}$  source was used to illuminate a 300  $\mu m$  deep, 50  $\mu m$  pitch Enertec SMD<sup>6)</sup>. The gate was provided by 2 plastic scintillators placed in coincidence. The defining counter had a width  $a=2.54$  cm placed at a height  $h = 10$  cm above the source. The maximum angle of incidence to the SMD is then  $\pm 127$  mrad. Since the SMD is  $\sim 2.5$  cm above the source, the number of strips illuminated is  $\sim (50 \mu m / 25400 \mu m)^4 = (.008)^{-1}$ .

The SMD amplifier chain simulates the standard readout scheme; an MSP1 preamp driving twist and flat cable terminated in a 733 amp followed by a discriminator set at threshold  $V_T$ . In figure 5 is shown the coincidence ratio  $S1.T/S1$  for various bias voltages  $V_D$ . Full depletion appears to be achieved at  $\sim 60$  volts bias. Hence,  $V_D$  was set to 100 volts.

Having set  $V_D$  for full depletion, one expects a charge collection time of  $t_c \sim 9.0$  nsec (for holes). In Figure 6 the coincidence ratio vs delay time is shown. A total timing jitter of 12 nsec is observed. This jitter is due to both phototube, SMD, and electronics. Clearly, the total jitter which is observed is such that  $> 25$  nsec coincidence gates can be used if the SMD is to operate in a digital mode.

The singles rate of a strip is shown in Figure 7 as a function of  $V_T$ . The noise rate is an exponential function of  $V_T$  with a noise exponent  $V_T^n = 5.65$  mV. If one sets  $V_T = 100$  mV then the rate is  $\sim 200$  HZ/strip. For 1000 strips (5 cm wide, 50  $\mu$ m pitch) the noise rate/plane would be 200 kHz. With a 50 nsec gate width, the accidental probability/plane would be 1%. Adopting 200 mV as corresponding to 30,000 q then 5.65 mV means ENC  $\sim 850$  q. This figure is roughly what is expected for this readout chain as mentioned above.

Finally, the pulse height spectrum gated on  $S=S1.S2$  is shown in Figure 8. The exponential noise spectrum is clear in Fig. 8a which is a log plot. Clearly a usable signal appears, with a peak observable in the linear plot of Figure 8b. Note that charge sharing over strips has not been removed by the device of vetoing on hits in adjacent strips. Such a bias would be unrealistic since under experimental conditions the SMD will be uniformly illuminated.

#### References

- 1) a) Silicon Detectors for High Energy Physics, ed. T. Ferbel, Fermilab October 15-16, 1981
- b) G. Charpak and F. Sauli, Ann. Rev. Nuc. Part. Sci. 34, 285 (1984).
- c) Vertex Detectors: Charm and Beauty I, Fermilab September 21-22, 1984.
- 2) The Art of Electronics, P. Horowitz and W. Hill, Cambridge University Press, 1980.
- 3) P. D'Angelo et al., Nuc. Inst. and Meth. 193, 533 (1982).



- 4) Micron Semiconductor Inc., 126 Baywood Ave., Longwood, Florida (305)339-4365.
- 5) J.P. Avondo et. al., Nucl. Inst. and Meth. in Phys. Res. A241, 107 (1985).
- 6) Courtesy of E-691 (on loan).

#### Figure Captions

- 1) Card cage from E-691 (TPL) to hold preamps and connect to microstrip detector.
- 2) Dimensions and pinouts of the CERN MSP1 preamp.
- 3) Schematic layout of SMD, preamp, and amplifier/discriminator.
- 4) Layout of the system test.
- 5) Coincidence ratio vs SMD bias voltage for  $V_T=100$  mV.
- 6) Coincidence ratio vs delay time for  $V_T=100$  mV,  $V_D=100$  V.
- 7) SMD singles rate/strip for various thresholds  $V_T$ .
- 8) Pulse height of detector with gate =  $S = S_1 \cdot S_2$ .
  - a) Log plot showing exponential noise fallout with pulse height and the residual signal.
  - b) Linear plot showing ~ 2:1 peak/valley.

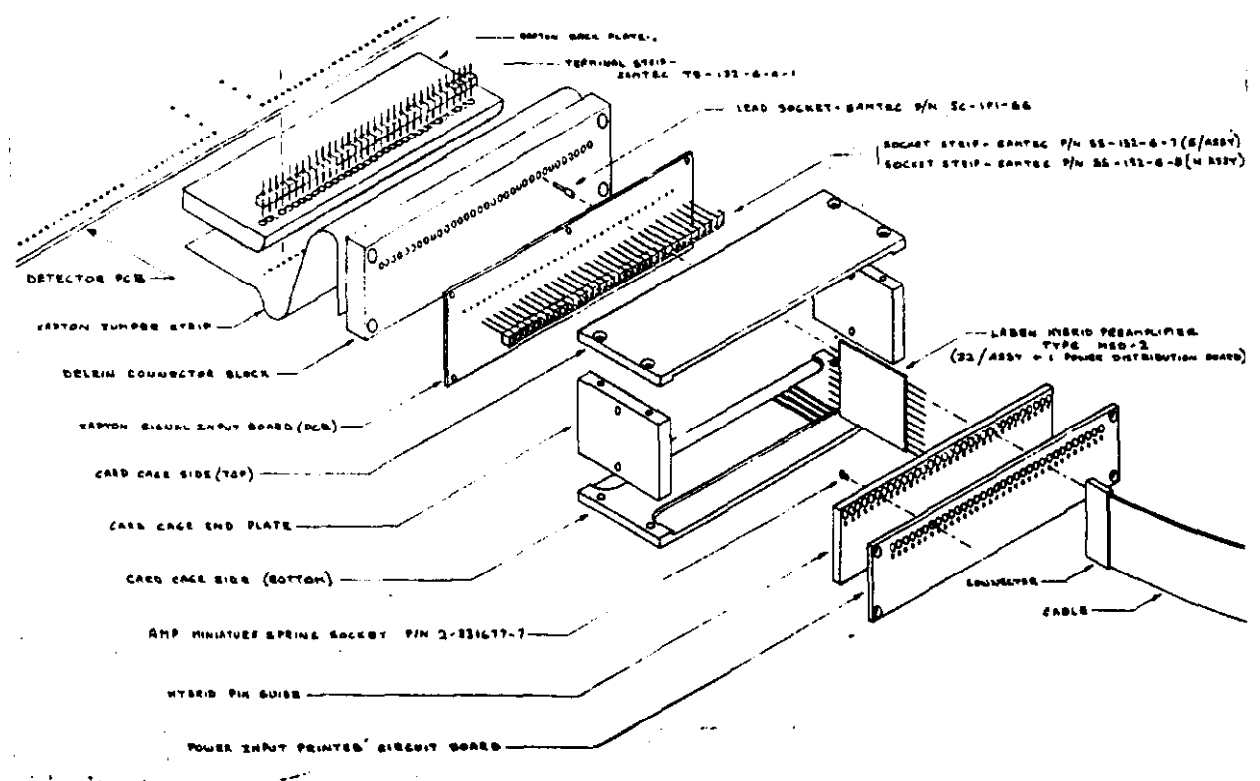
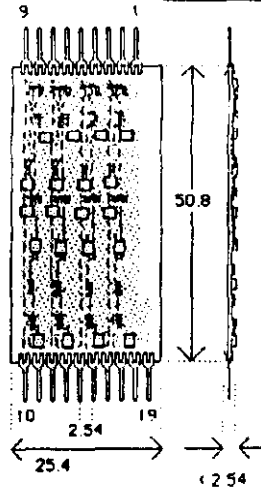


Figure 1

# MECHANICAL CONFIGURATION



- |             |                             |
|-------------|-----------------------------|
| 1 - GROUND  | 10 - -Vcc (-6)              |
| 2 - INPUT 1 | 11 - NON INVERTING OUTPUT 4 |
| 3 - GROUND  | 12 - INVERTING OUTPUT 4     |
| 4 - INPUT 2 | 13 - NON INVERTING OUTPUT 3 |
| 5 - GROUND  | 14 - INVERTING OUTPUT 3     |
| 6 - INPUT 3 | 15 - NON INVERTING OUTPUT 2 |
| 7 - GROUND  | 16 - INVERTING OUTPUT 2     |
| 8 - INPUT 4 | 17 - NON INVERTING OUTPUT 1 |
| 9 - GROUND  | 18 - INVERTING OUTPUT 1     |
|             | 19 - +Vcc (+6)              |

## BLOCK DIAGRAM

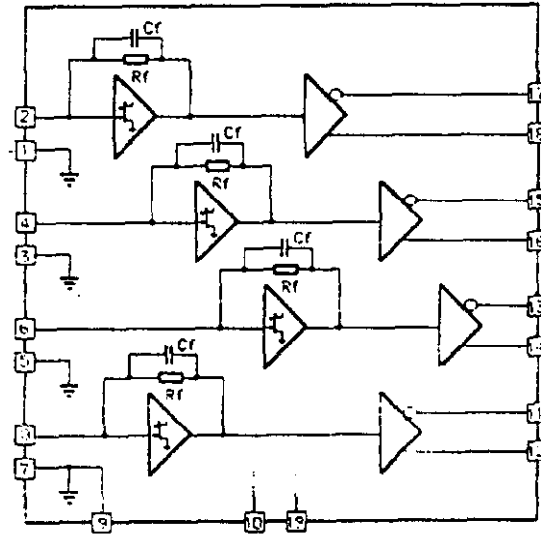


Figure 2

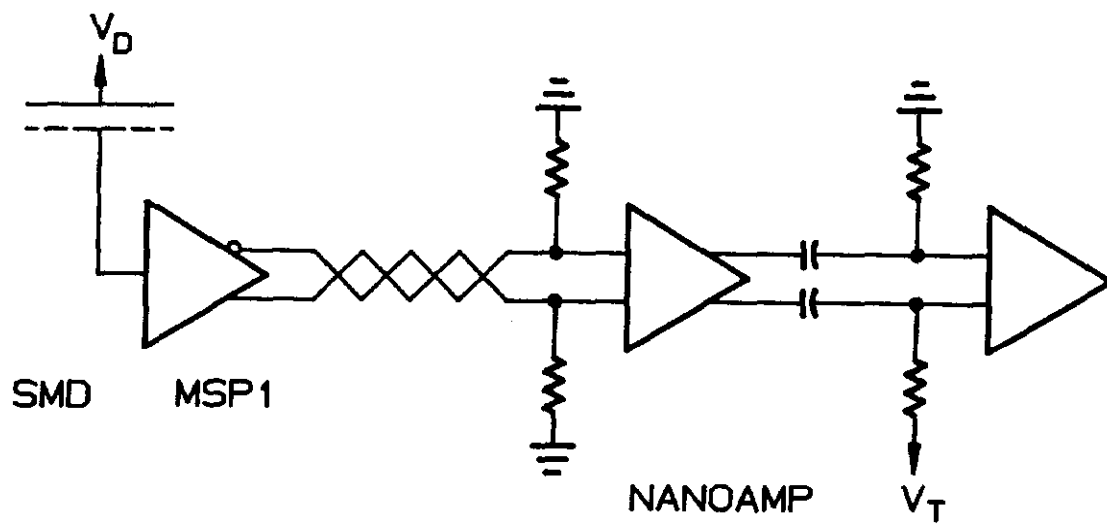


Figure 3

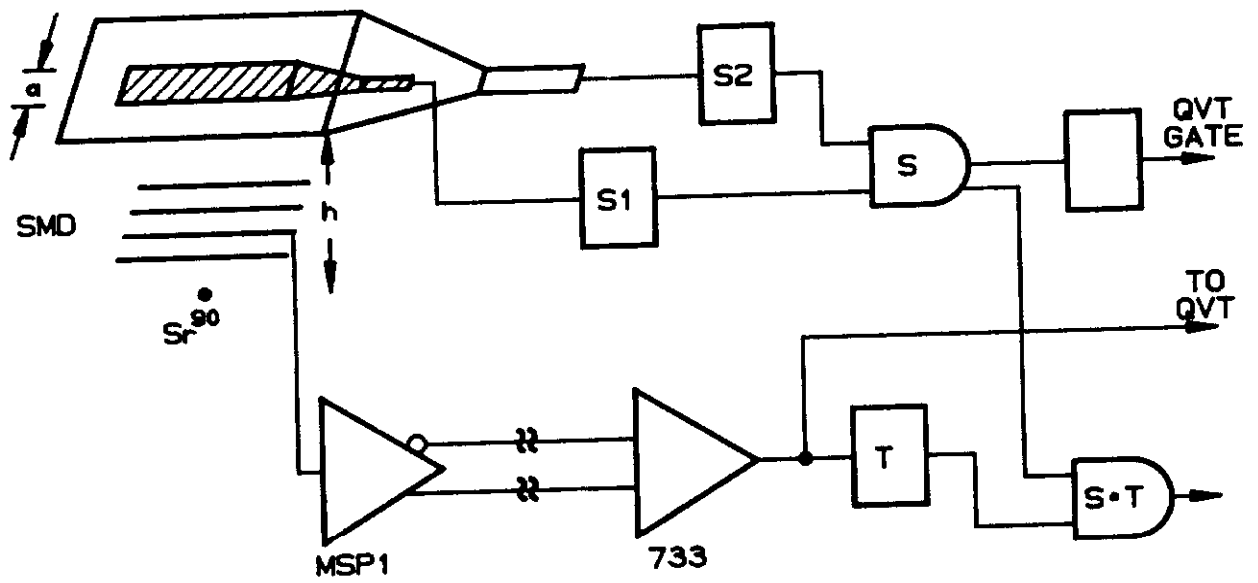


Figure 4

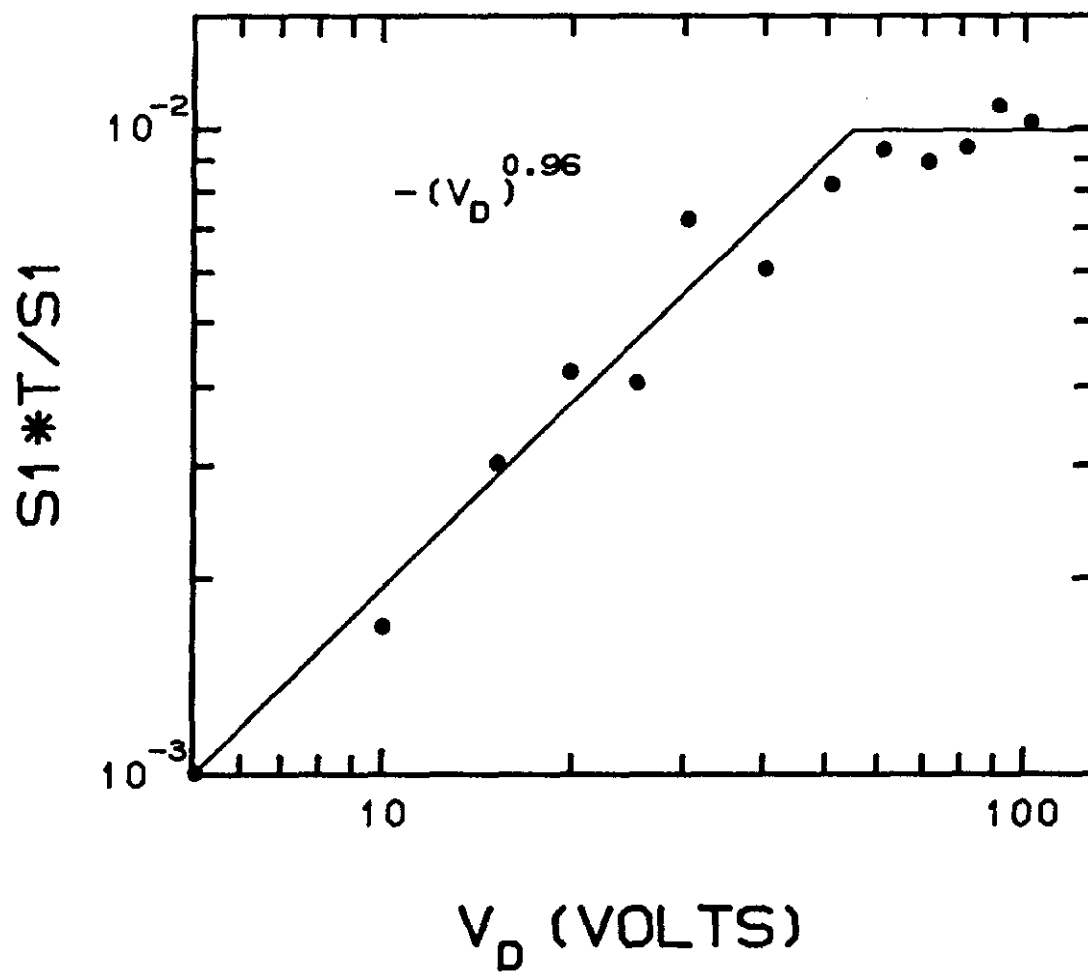


Figure 5

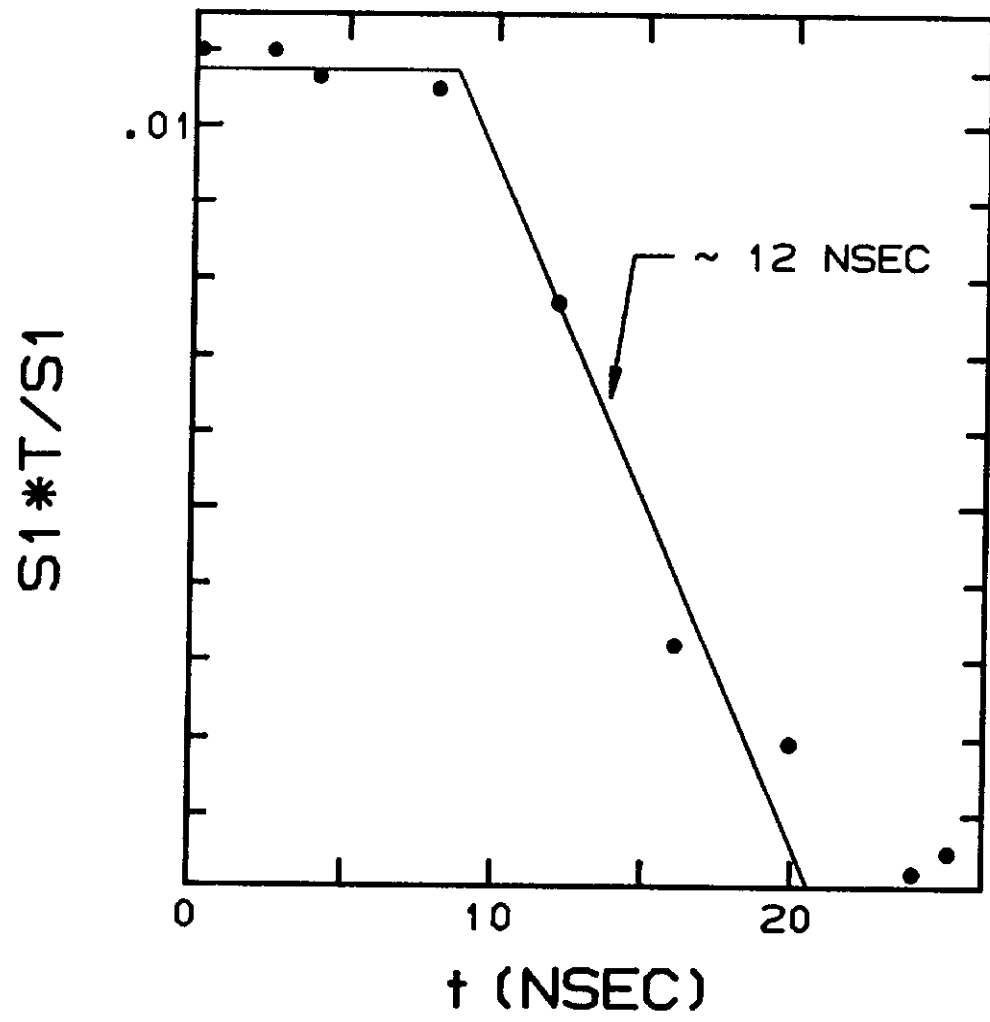


Figure 6

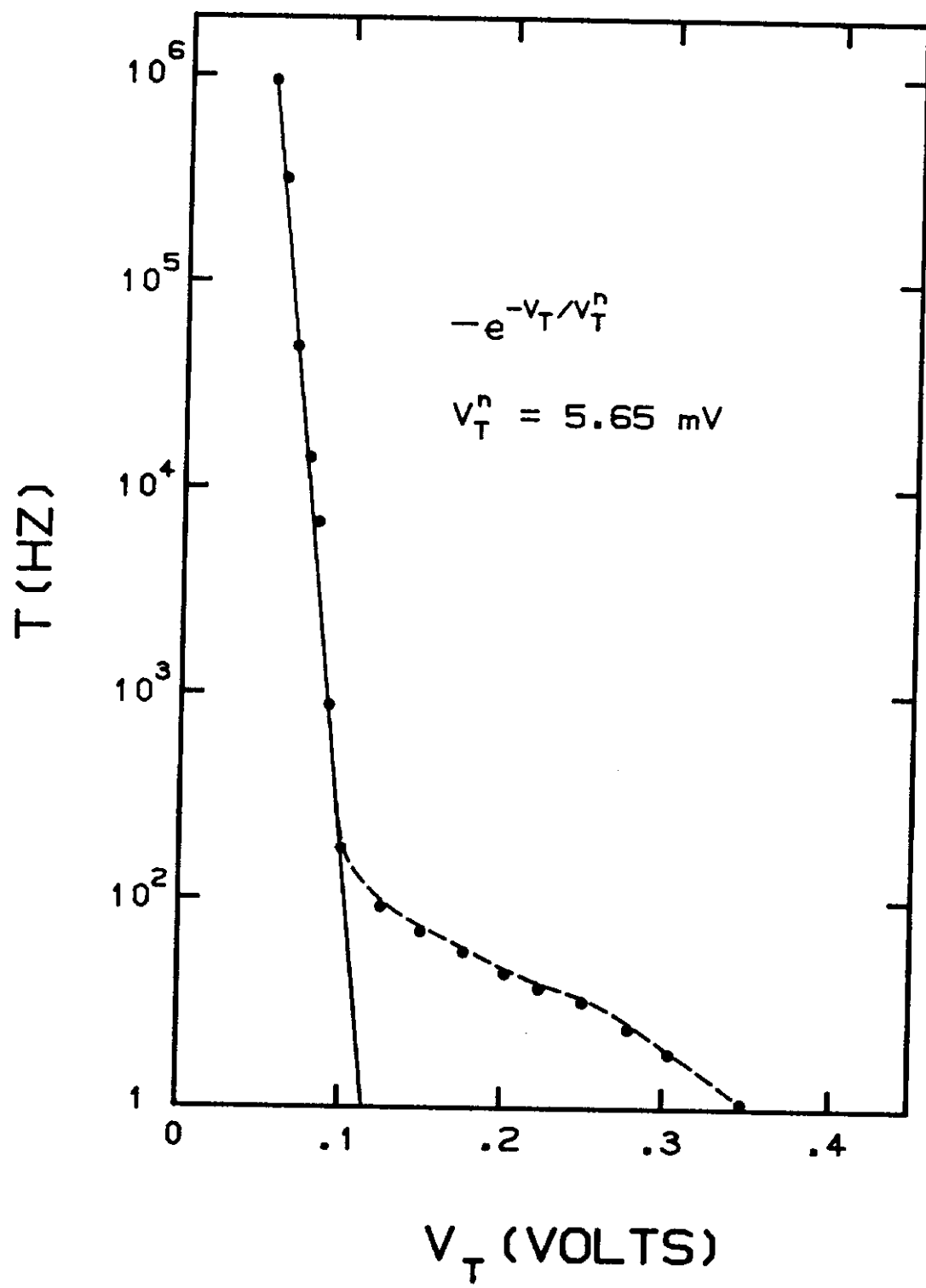
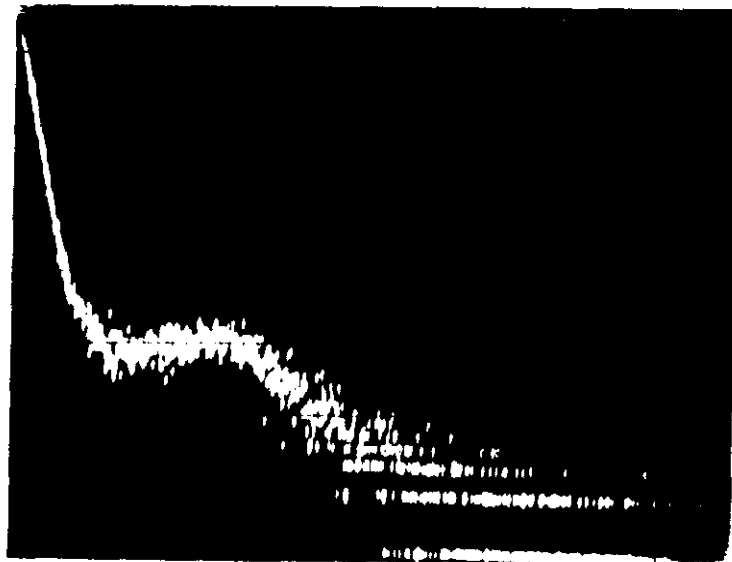
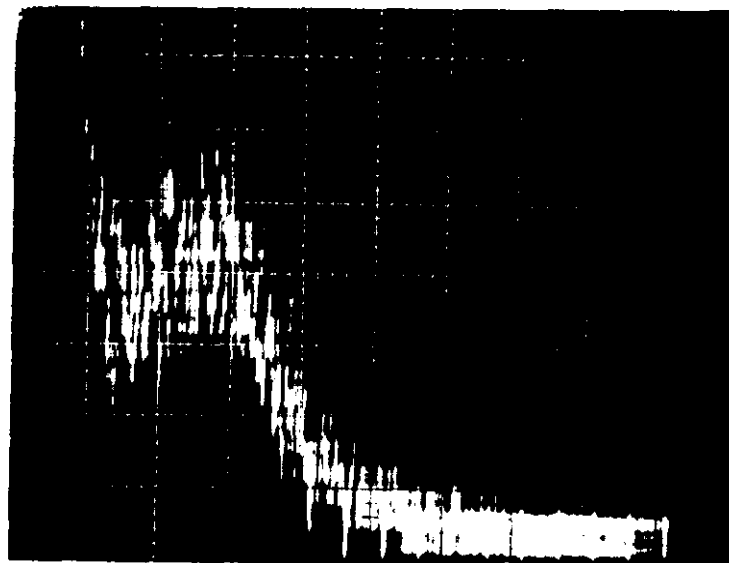


Figure 7





a)



b)

Figures 8a and 8b